



# CO<sub>2</sub> Capture for Dry Reforming of Natural Gas: Performance and Process Modeling of Calcium Carbonate Looping Using Acid Based CaCO<sub>3</sub> Sorbent

Muhammad Afiq Zubir<sup>1,3</sup>, Nurfanizan Afandi<sup>2</sup>, Abreeza Manap<sup>2\*</sup>, Awaluddin Abdul Hamid<sup>4</sup>, Bamidele Victor Ayodele<sup>2</sup>, Wen Liu<sup>5</sup> and Mohd Kamaruddin Abd Hamid<sup>1</sup>

<sup>1</sup>Process Systems Engineering Centre (PROSPECT), Research Institute for Sustainable Environment (RISE), Universiti Teknologi Malaysia, Johor, Malaysia, <sup>2</sup>College of Engineering, Institute of Sustainable Energy (ISE), Universiti Tenaga Nasional, Kajang, Malaysia, <sup>3</sup>UNITEN R&D Sdn. Bhd., Universiti Tenaga Nasional, Kajang, Malaysia, <sup>4</sup>Tenaga Nasional Berhad (TNB), Seri Manjung, Malaysia, <sup>5</sup>School of Chemical and Biomedical Engineering, Nanyang Technological University, Nanyang, Singapore

## OPEN ACCESS

### Edited by:

Simona Liguori,  
Clarkson University, United States

### Reviewed by:

Sang-Sup Lee,  
Chungbuk National University,  
South Korea  
Noah McQueen,  
University of Pennsylvania,  
United States

### \*Correspondence:

Abreeza Manap  
abreeza@uniten.edu.my

### Specialty section:

This article was submitted to  
Advanced Clean Fuel Technologies,  
a section of the journal  
Frontiers in Energy Research

**Received:** 26 September 2020

**Accepted:** 18 December 2020

**Published:** 22 January 2021

### Citation:

Zubir MA, Afandi N, Manap A, Hamid AA, Ayodele BV, Liu W and Abd Hamid MK (2021) CO<sub>2</sub> Capture for Dry Reforming of Natural Gas: Performance and Process Modeling of Calcium Carbonate Looping Using Acid Based CaCO<sub>3</sub> Sorbent. *Front. Energy Res.* 8:610521. doi: 10.3389/fenrg.2020.610521

Several industrial activities often result in the emissions of greenhouse gases such as carbon dioxide and methane (a principal component of natural gas). In order to mitigate the effects of these greenhouse gases, CO<sub>2</sub> can be captured, stored and utilized for the dry reforming of methane. Various CO<sub>2</sub> capture techniques have been investigated in the past decades. This study investigated the performance and process modeling of CO<sub>2</sub> capture through calcium carbonate looping (CCL) using local (Malaysia) limestone as the sorbent. The original limestone was compared with two types of oxalic acid-treated limestone, with and without aluminum oxide (Al<sub>2</sub>O<sub>3</sub>) as supporting material. The comparison was in terms of CO<sub>2</sub> uptake capacity and performance in a fluidized bed reactor system. From the results, it was shown that the oxalic acid-treated limestone without Al<sub>2</sub>O<sub>3</sub> had the largest surface area, highest CO<sub>2</sub> uptake capacity and highest mass attrition resistance, compared with other sorbents. The sorbent kinetic study was used to design, using an Aspen Plus simulator, a CCL process that was integrated with a 700 MWe coal-fired power plant from Malaysia. The findings showed that, with added capital and operation costs due to the CCL process, the specific CO<sub>2</sub> emission of the existing plant was significantly reduced from 909 to 99.7 kg/MWh.

**Keywords:** CO<sub>2</sub> capture, calcium carbonate, natural gas, process modeling, economic analysis

## INTRODUCTION

Global climate change has remained as one of the major environmental issues of the past decades. Human activities such as the burning of fossil fuels, industrial processes, and various land uses have significantly contributed to the release of greenhouse gases (GHGs) such as carbon dioxide (CO<sub>2</sub>) and methane (CH<sub>4</sub>) into the atmosphere. According to Anderson and Newell (2004), CO<sub>2</sub> is the most dominant gas of the released GHGs. The increase in CO<sub>2</sub> emissions will cause an overabundance of greenhouse gases that trap additional heat. Consequently, it will cause the Earth's temperature to increase, which will melt the ice at the poles and lead to the rise of sea level. The largest contributors to CO<sub>2</sub> gas emissions are power plant industries (Abeydeera et al., 2019) and they account for a third

of the total greenhouse gas emissions (International Energy Agency, 2016a). Around 40.8% of these industries generate coal-based electricity (International Energy Agency, 2016b). Currently, the transition to cleaner and more sustainable energy systems is sluggish. Even though there have been efforts to use renewable energy for electricity generation, the use of fossil fuels remains high, up to 66.7% (International Energy Agency, 2016b). To cope with this, carbon tax has been implemented in several countries in hope to reduce the CO<sub>2</sub> emissions by 40–65% by 2030 (Zhang et al., 2017; Cui et al., 2019; Akerboom et al., 2020). The aim of this tax is to motivate the industries to reduce their carbon emissions through research and development (R&D) on applicable carbon capture technologies. One major route to technically utilize both CO<sub>2</sub> and CH<sub>4</sub> is through reforming process. However, it is expedient to examine how the CO<sub>2</sub> can be captured and store for subsequent utilization in dry reforming of natural gas.

A number of R&D activities have been done on carbon capture and storage technologies. For pre-combustion capture, an integrated gasification combined cycle (IGCC) has been proposed, through which fossil fuels will be gasified into a high pressure synthesis gas (syngas) before steam is injected to extract CO<sub>2</sub> gas through a series of catalyst beds (Carpenter et al., 2017). For post-combustion capture, one of the most commercialized technologies is wet scrubbing with an aqueous solution of monoethanolamine (MEA) (Wang et al., 2017). Another common technology is oxy-fuel combustion process, through which fuel is burnt in a mixture of oxygen and recycled flue gas. The absence of nitrogen in the combustion process produces exhaust gas with high CO<sub>2</sub> concentrations and enables easier purification (Hou et al., 2020). The main drawback of this process is the huge energy required to run the air separation unit that would produce the oxygen needed for the combustion (Xiong et al., 2014).

Out of all technologies, Calcium Carbonate Looping (CCL) is one of the most promising technologies for large-scale CO<sub>2</sub> capture processes (Zhou et al., 2019). CCL is a post-combustion carbon capture technology that utilizes a solid CaO-based sorbent, which is natural limestone, to remove CO<sub>2</sub> from flue gasses at high temperatures. A CCL plant mainly consists of carbonation and CO<sub>2</sub> calcination. The major pieces of equipment used in the design of this plant can be divided into three systems, 1) reactors (carbonator and calciner); 2) separators (cyclones); and 3) heat networks (heat exchangers). One of the advantages of using CCL is that it utilizes a widely available and inexpensive sorbent, unlike other technologies (Mantripragada and Rubin, 2014). CCL offers the possibility of generating extra power through steam generation by using the tremendous amount of excess heat from high-temperature carbonation and calcination reactions of solid calcium oxide (CaO) sorbents (Hilz et al., 2019). It also has potentially lower energy penalties and less toxicity than amine scrubbing (Ströhle et al., 2015). In addition, the application of this technology has been carried out rapidly on various scales and at various operating configurations, from 3 kWth up to 1.9 MWth (Charitos et al., 2010; Arias et al., 2013; Chang et al., 2013). Despite that, this technology faces a major problem that is the

degradation of the sorbent used in the CCL process. The degradation of sorbent is mainly due to the structure of sorbent that is not stable at high temperature and causes the strength of sorbent to be degraded. Over the years, many studies have been carried out to improve the sorbent performance in the CCL process. Example of improvements include the use of water as a reactivation agent for the sorbent (Ramkumar and Fan, 2010; Mutch et al., 2017), salt doping (Sun et al., 2012; Erans et al., 2018), thermal pre-treatment (Valverde et al., 2017), and acid pre-treatment (Ridha et al., 2013).

The durability of sorbent can be enhanced by reinforcing or doping the limestone with supported material. Florin and Fennell (2011) found that aluminum as supported material can increase the strength of sorbent hence increase the durability of sorbent material in CCL process. Radfarnia and Iliuta (2013) also reported that using aluminum as supported material has higher CO<sub>2</sub> uptake than Zirconia, Yttrium and Magnesium. Besides that, the usage of acid or acid pre-treatment can increase the CO<sub>2</sub> carrying capacity and reactivity of limestone. Miranda-Pizarro et al. (2017) was investigating the CaO-based sorbents using acetic acids and found that the presence of acetate could reduce the energy penalty by lowering the temperature needed in calciner operation. Moreover, Ridha et al. (2013) studied that sorbents treated with oxalic acid was found to have good CO<sub>2</sub> absorption capacity compared to other organic acids such as formic acid, and vinegar. Oxalic acid increases the sorbent's porosity and surface area, thus increasing CO<sub>2</sub> absorption capacity compared to other acid-treated sorbents.

Therefore, the objective of this research is to investigate the performance of sorbent prepared from Malaysian limestone treated with oxalic acid, with and without aluminum as supporting material, and to conduct a performance and process modeling study of a coal-fired power plant (Malaysia), in which is installed a calcium looping process that uses oxalic-acid treated limestone. The sorbents' CO<sub>2</sub> uptake capacity and performance were analyzed using a fluidized bed reactor system. Then, the sorbent with the highest CO<sub>2</sub> uptake capacity was selected to be studied in more detail before it was integrated with the coal-fired power plant in the Aspen simulator. Lastly, a preliminary economic analysis was carried out to compare the capital and operation costs of the existing power plant and the integrated CCL-power plant, based on the selected sorbent. Since there is abundant natural gas research, the CO<sub>2</sub> captured is proposed to be used for natural gas reforming to produce synthetic gas.

## TECHNICAL DESCRIPTION

### Reference Coal-Fired Power Plant (Without Calcium Carbonate Looping Process)

A 700 MWh<sub>e</sub> industrial coal-fired power plant was used as reference for this study. The referenced plant consists of several major pieces of equipment, as shown in **Figure 1**. Initially, coal is grinded to obtain particles of sizes around 75 μm. Force draught (FD) air and primary air (PA) are pre-heated using a rotary air heater (RAH) before they are fed into a combustion chamber together with the grinded coal. The flue gas

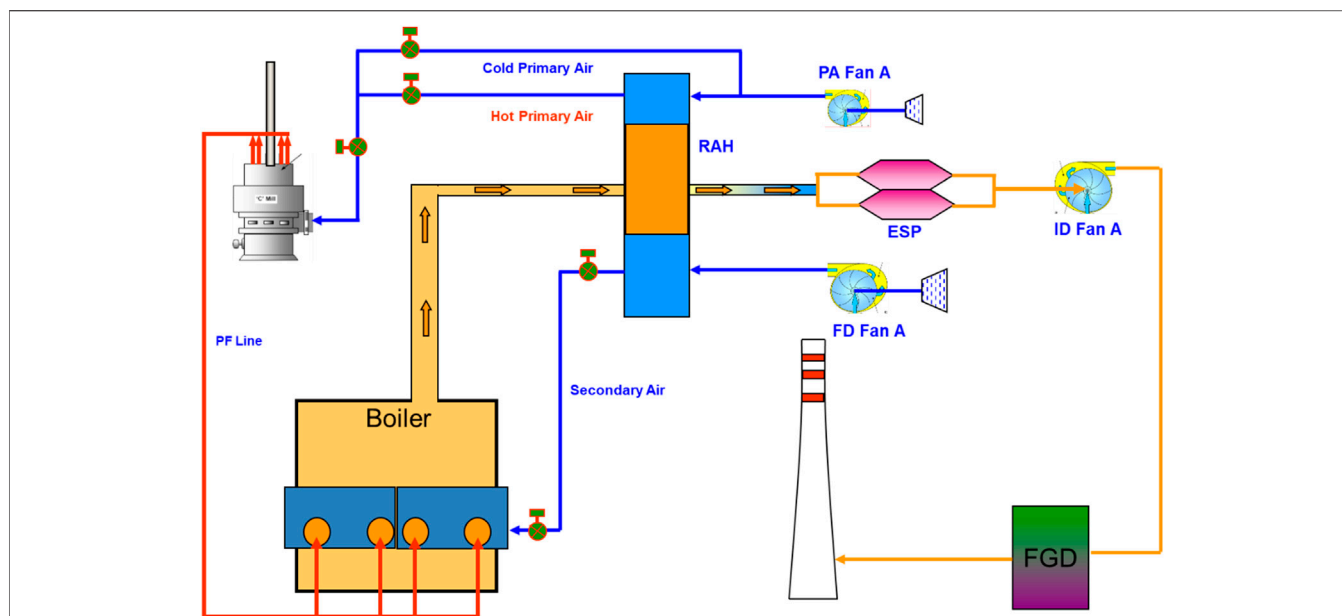


**FIGURE 1 |** Process Flow Diagram (PFD) of the reference plant: Primary air is supplied to the pulverizer through Primary Air Fan A (PA Fan A). The combined pulverized coal and air is fed to the boiler through Primary Fan Line (PF Line) before it is mixed with the additional air supplied to the boiler from Force Draft Fan A (FD Fan A). The hot flue gas generated from the boiler is used to preheat the air feed of the boiler using the Rotary Air Heater (RAH). Dust in the flue gas is removed in an Electrostatic Precipitator (ESP) before it passes through the installed Induced Fan A (ID Fan A) to maintain a negative pressure in the boiler. The flue gas is then processed in the Flue Gas Desulphurization (FGD) to reduce the sulfur content in the flue gas before the gas is removed through the stack.

**TABLE 1 |** General information on the referenced plant.

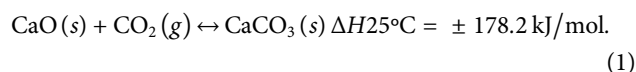
Parameters	Value
Excess air (%)	15
Amount of coal used (ton/h)	335.77
Ultimate analysis (%)	
Ash	4.15
Carbon	66.28
Sulfur	0.37
Oxygen	29.20
Super-heater	
Pressure (bar)	177.8
Temperature (°C)	540.3
Re-heater	
Pressure (bar)	35.6
Temperature (°C)	543.1
Economiser exit temperature (°C)	321.2
Polytrophic efficiencies of turbines (%)	
High pressure (HP)	84.8
Medium pressure (MP)	92.5
Low pressure (LP)	85.0

produced from the combustion are cooled through heat transfer in a superheater, reheater, and economiser through a series of heat exchangers. The flue gas is further cooled in the RAH before they enter an Electrostatic Precipitator (ESP) for the removal of ashes that remain in the flue gas. The flue gas is then exhausted using an induced draught fan into a flue gas desulphurization (FGD) system for  $\text{SO}_x$  removal. Seawater is used as the medium in the absorber of the FGD system. It is removed through the bottom of the absorber whilst the cleaned flue gas exits the top of the absorber and is transferred to the stack.

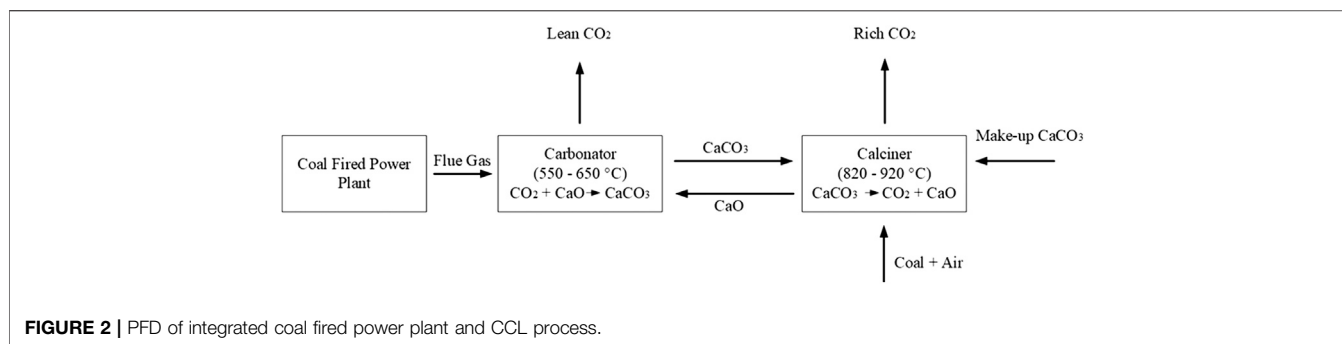
The referenced plant utilizes conventional three-stage turbines that consist of a single High Pressure (HP) turbine, a single Medium Pressure (MP) turbine, and a double Low Pressure (LP) turbine. The general information on this plant is shown in **Table 1**. The referenced plant was simulated using Aspen Plus simulator based on actual plant data and was compared with a CCL process-integrated plant in terms of capital cost, operation cost, and  $\text{CO}_2$  emission per MWh.

## Calcium Carbonate Looping Process

The objective of a calcium carbonate looping (CCL) plant is to capture the  $\text{CO}_2$  in the flue gas of the referenced plant before the gases are released to the surroundings through a stack. Initially, the CCL process is carried out in a small-scale laboratory to compare the performance of modified calcium carbonate sorbents. The best sorbent is then chosen for the simulation of an actual-size CCL process for the flue gas from the referenced plant. Since the flowrate of the flue gas is too huge, the CCL process is divided into two process lines. Each process line consists of two interconnected fluidized bed reactors: a carbonator and a calciner, as shown in **Figure 2**. The common carbonator and calciner reactors' operating temperatures are 550–650 °C and 820–920 °C (Ridha et al., 2013), respectively. The main reaction involved in the CCL process is:



The (exothermic) forward reaction that uses the  $\text{CO}_2$  in the flue gas to form solid calcium carbonate ( $\text{CaCO}_3$ ) occurs in the



carbonator reactor whilst the (endothermic) backward reaction that converts solid  $\text{CaCO}_3$  back to gaseous  $\text{CO}_2$  and calcium oxide ( $\text{CaO}$ ) after the separation of flue gas in the cyclone separators is favored in the calciner reactor. Heat from the oxy-fuel combustion (that was proposed by Rolfe et al. (2018)) is supplied to the calciner reactor. Then, the  $\text{CaO}$  is recycled back into the carbonator reactor for a continuous operation. A small amount of make-up pure  $\text{CaCO}_3$  is fed into the calciner reactor to compensate for the loss of sorbent due to side reactions in the carbonator reactor and separation processes in the CCL. According to Rolfe et al. (2018),  $\text{CO}_2$  absorption rates of up to 90% can be achieved through the process.

The heat from the lean  $\text{CO}_2$ -flue gas stream leaving the carbonator and the concentrated  $\text{CO}_2$  gas from the calciner is used to generate additional steam for power generation in the referenced plant. The specifications of the steam generated from the additional heat is set similar to the referenced plant's steam specifications shown in **Table 1**.

## METHODOLOGY

### Materials and Sample Preparation

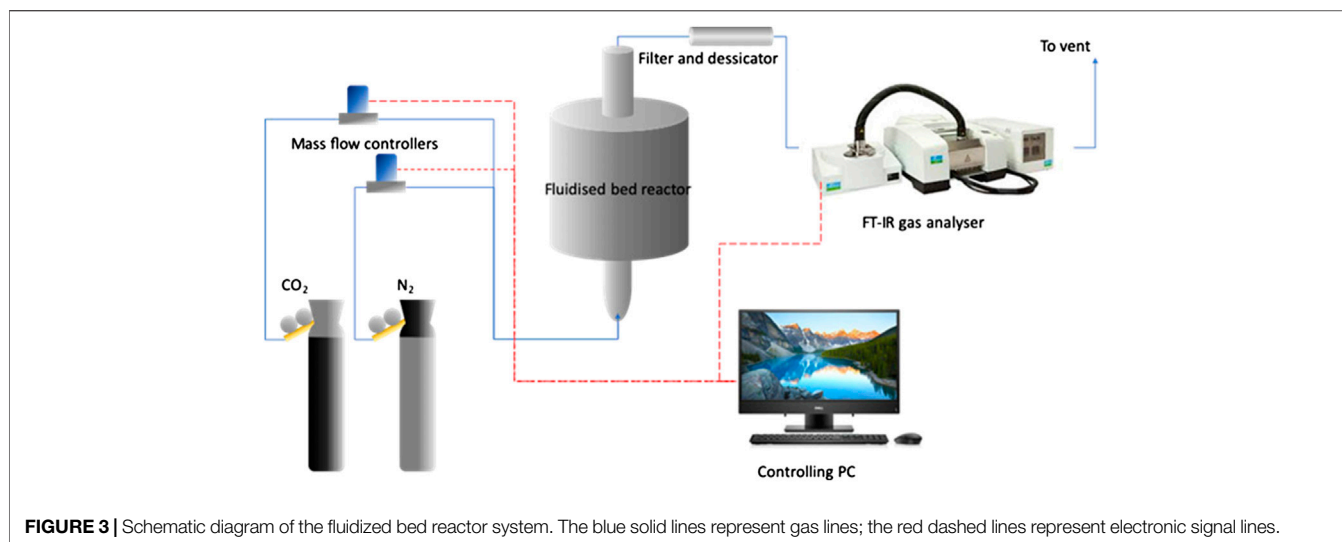
The fresh limestones were obtained from GCCP Resources (Malaysia) and the supported materials; aluminum nitrates was obtained from Sigma Aldrich (United States). The fresh limestones were mechanically ground and sieved to a particle size less than 1 mm using laboratory grinder at Universiti Tenaga Nasional (UNITEN), Malaysia. The sieved limestone, weighing approximately 20 g, was mixed with aluminum nitrate at ratio of 80:20. The mixture was mixed using the stirring hot plate (FAVORIT, HS0707V2) at temperature of 100 °C for 5 min. Then the oxalic acid was mixed at concentration of 1.0 M. For oxalic acid-treated limestone without supporting material, the oxalic acid was mixed with limestone prior to heating. Next, it was heated inside a furnace (TDW KSW-6-16) at 300 °C for 1 h and later cooled down at room temperature for 24 h to obtain the desired sorbents.

The surface area and pore volume size were calculated using Brunauer-Emmett-Teller (BET; Micromeritics ASAP 2020). The total pore volume was estimated from the amount of nitrogen adsorbed at  $P/P_0 = 0.200$ . Gas analysis was performed by a FTIR (PerkinElmer, Frontier MIR) equipped with a gas cell which is

originally designed for TG-IR analysis. The gas cell has an optical path length of ca. 13 cm. Sampling was achieved by a sampling pump drawing flue gas from the fluidized bed reactor at a rate of 0.5 L/min (STP). **Figure 3** shows a schematic diagram of fluidized bed reactor that was used in this study.

### $\text{CO}_2$ Absorption Performance

The  $\text{CO}_2$  uptake capacity was analyzed using Thermogravimetric Analysis (TGA) (Mettler Toledo TGA/DSC2 LF/1100/203). In this study, the carbonation-calcination cycles in a TGA were simulated by isothermal concentration swings (switching between  $\text{CO}_2$  and  $\text{N}_2$ ) at 750 °C. The isothermal cycles were used to implement the generalized methods of kinetic analysis (Fedunik-Hofman et al., 2019). Then, the performance of the synthetic sorbent such as cyclic  $\text{CO}_2$  uptake capacity over 100 cycles of carbon capture, sorbent attrition rate and reaction kinetics were investigated using the batch bubbling fluidized bed reactor as shown in **Figure 3**. The powder of sorbents was pelletized in a 13 mm I.D. stainless steel die using a hydraulic press at a force of 1 kN. The pelletized sorbents were broken into fragments and sieved to the size range of 0.8–1.0 mm. At pilot scale, the process of interest is deployed in the form of a circulating fluidized beds system with a dual bubbling bed design, in which solid circulation is achieved through particle entrainment by stand pipes inserted into the fluidized beds. In each experiment, ~15.0 ml of quartz sand (210–300  $\mu\text{m}$ , purchased from Sigma Aldrich without further purification) was used as the main bed material. During carbonation-calcination cycles, the bed operated isothermally at 750 °C, which was achieved by external heating by a tubular furnace with a uniform temperature zone as long as 400 mm. The fluidizing gas was either pure  $\text{N}_2$  (for calcination) or 15%  $\text{CO}_2$  in  $\text{N}_2$  (for carbonation). The 15%  $\text{CO}_2$  concentration is chosen to mimic the flue gas concentration from a coal-fired power plant. At all times, the total flowrate of the fluidizing gas is kept at ~1.00 L/min (as measured at 298 K and 1 atm pressure), which corresponds to  $U/U_{mf}$  of approximately 6.6 at the operating temperature of 750 °C, assuming white sand density of 3,000  $\text{kg m}^{-3}$ . Each carbon capture cycle consists of 8 min carbonation (15%  $\text{CO}_2$  in  $\text{N}_2$ ) and 8 min calcination (pure  $\text{N}_2$ ). In each experiment, approximately 1.0 g of  $\text{CaO}$  sorbent sample was cycled 100 times isothermally at 750 °C. It was conducted so because in the batch, fluidized bed-calcium



looping experiments, it was practically impossible to achieve instantaneous temperature swings between 650 and 920 °C in a single carbonation-calcination cycle. This limitation made kinetic measurement difficult. Therefore, a more feasible method was performed, which was isothermal cycles at 750 °C, by using 15% CO<sub>2</sub> as the simulated flue gas and N<sub>2</sub> for calcination. This method has been widely adopted in the existing pieces of literature for examining the cyclic stability of Ca-based sorbents (Stendardo et al., 2013; Ramezani et al., 2017; Fedunik-Hofman et al., 2019). The sorbent particles, after the cycling experiment, was recovered by sieving and weighed again to determine the extent of attrition.

### Preliminary Economic Analysis

The purpose of this analysis is to compare the economics of the referenced plant with the integrated plant. Their operating costs were estimated from the costs of utility, raw materials, maintenance and labor. The maintenance and labor cost was considered as 5% of the capital cost of the plant (Sinnott and Towler, 2020). The capital estimation included the cost of equipment and its installation, based on the cost factor retrieved from Sinnott and Towler (2020). Only major pieces of equipment were considered for the equipment cost, and the prices of the pieces were estimated using simple equations obtained from Michalski et al. (2019) because of the minimal input they require. The equations were initially in Euro, so for this study, they were converted to USD with a factor of 1.0898 USD/Euro taken on Mei 2020. Carbon steel was assumed as the construction material. The costs of reactors were estimated using the following Eqs. 2, 3, which are based on the reactors' heat usage (Q, kW).

$$\text{Cost of carbonator reactor (USD)} = 18,080 \times Q_{\text{car}}^{0.67}, \quad (2)$$

$$\text{Cost of calciner reactor (USD)} = 14,320 \times Q_{\text{cal}}^{0.67}. \quad (3)$$

For a heat exchanger, its surface area ( $A_{\text{Hex}}$ , m<sup>2</sup>) and operating pressure ( $P_{\text{Hex}}$ , bar) were used to estimate its prices, as shown in Eq. 4.

$$\text{Cost of heat exchanger (USD)} = 2775.52 \times A_{\text{Hex}}^{0.67} \times P_{\text{Hex}}^{0.28}, \quad (4)$$

The cost of a compressor was calculated based on its break power ( $P_B$ , kW) and isentropic efficiency ( $\eta_i$ ), as shown in Eq. 5.

$$\text{Cost of a compressor (USD)} = 3848.4xP_B^{0.71} \times \left[ 1 + \left( \frac{1 - 0.8}{1 - \eta_i} \right)^3 \right]. \quad (5)$$

The capital cost of a cyclone separator was calculated using Eq. 6, which was proposed by Seider et al. (2019). The flowrate of the inlet gas ( $Q_g$ , ft<sup>3</sup>/min) of a cyclone separator was used for the cost estimation.

$$\begin{aligned} \text{Cost of cyclone separator} = & \exp\{9.3485 - 0.7892[\ln(Q_g)] \\ & + 0.08487[\ln(Q_g)]^2\}. \quad (6) \end{aligned}$$

## RESULTS AND DISCUSSION

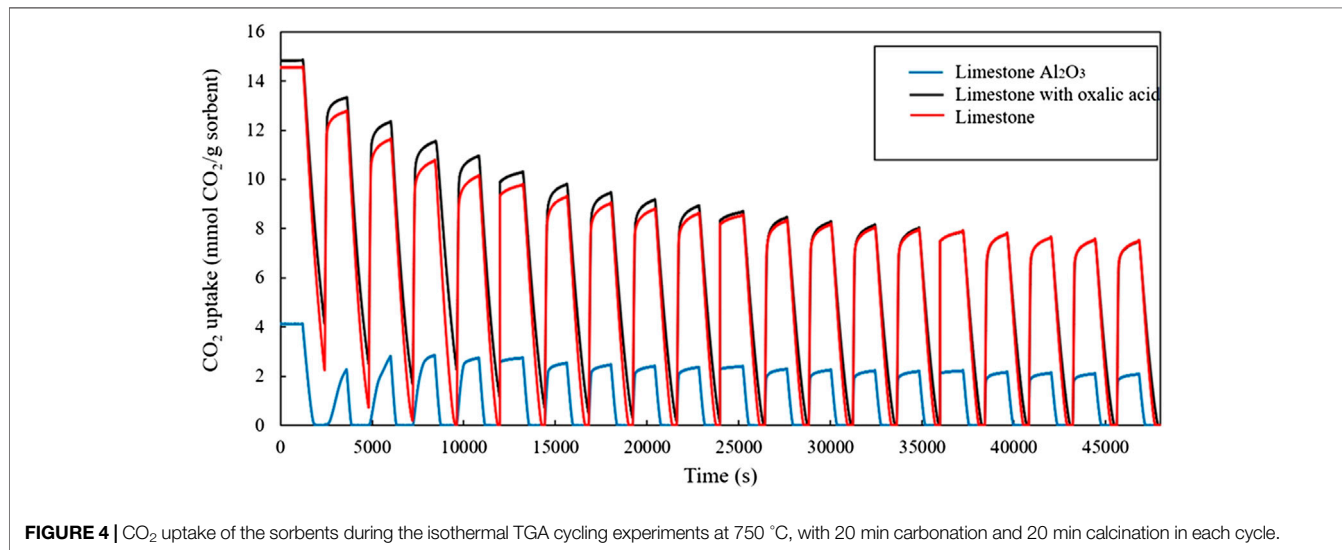
### Analysis of Sorbent

Table 2 shows the surface area and pore volume of non-treated limestone, oxalic acid-treated limestone, and oxalic acid-treated limestone with Al<sub>2</sub>O<sub>3</sub>. Limestone from Malaysia that are untreated with acid shows higher surface area and pore volume size which is 15.65 and 0.0537 m<sup>2</sup>/g, respectively, than Cadomin limestone, 5.2 m<sup>2</sup>/g (Ridha et al., 2013), limestone 9 m<sup>2</sup>/g (Li et al., 2009), limestone from Spain, 5 m<sup>2</sup>/g (Benitez-Guerrero et al., 2018) and Longcal limestone. <1 m<sup>2</sup>/g (Erans et al., 2018). After the treatment with oxalic acid, higher surface area was exhibited compared to non-treated limestone which is 17.01 m<sup>2</sup>/g. This value is in a good agreement with the reported surface area and pore volume size of Cadomin limestone treated with oxalic acid which exhibits higher surface area than using other organic acids such as formic acid and acetic acid (Ridha et al., 2013).



**TABLE 2** | Surface area and pore volume of limestone.

Sample no	Details of samples	Surface area (m <sup>2</sup> /g)	Pore volume (cm <sup>3</sup> /g)
1	Oxalic acid-treated limestone with Al <sub>2</sub> O <sub>3</sub>	3.113	0.014
2	Oxalic acid-treated limestone	17.01	0.067
3	Non-treated limestone	15.65	0.0537

**FIGURE 4** | CO<sub>2</sub> uptake of the sorbents during the isothermal TGA cycling experiments at 750 °C, with 20 min carbonation and 20 min calcination in each cycle.

Meanwhile limestone supported with Al<sub>2</sub>O<sub>3</sub> exhibit relatively lower surface area and pore volume. Although the current result shows that limestone supported with Al<sub>2</sub>O<sub>3</sub> reduce surface area and pore volume, this differs from previous findings where modification with Al<sub>2</sub>O<sub>3</sub> exhibits high surface area and pore volume size (Benitez-Guerrero et al., 2018; Przekop et al., 2018). To confirm this finding, second experiment was performed with the same method yielding the same result. This suggest that limestone type and origin could also be a factor that influences the final properties of the modified sorbent.

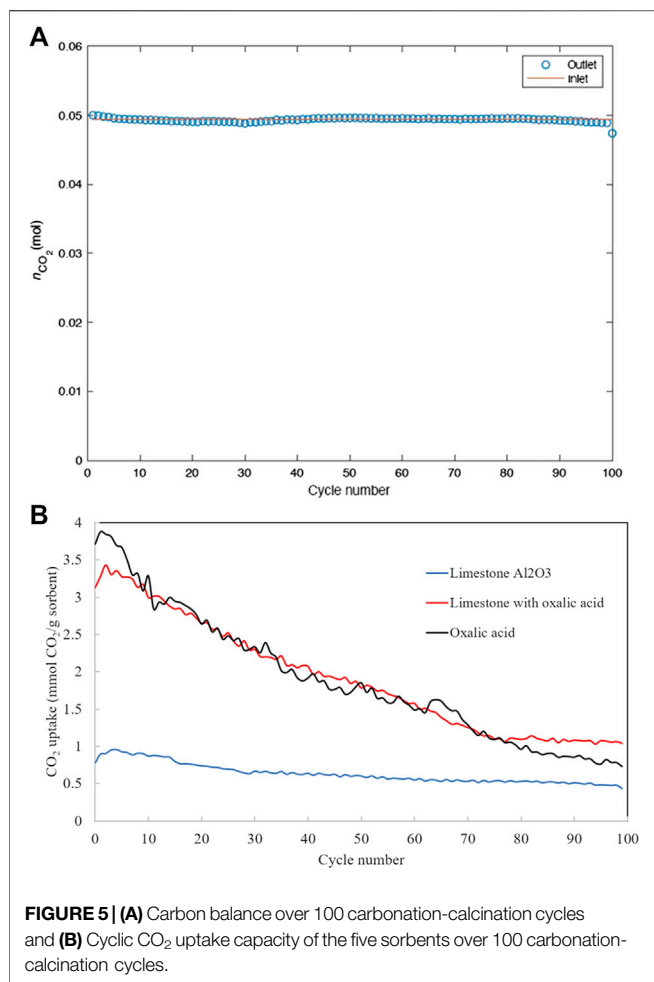
## CO<sub>2</sub> Capture Studies

**Figure 4** shows the CO<sub>2</sub> uptake capacity of non-treated limestone, oxalic acid-treated limestone, and oxalic acid-treated limestone with Al<sub>2</sub>O<sub>3</sub>. At the beginning, the non-treated limestone and oxalic acid-treated limestone have higher CO<sub>2</sub> uptake than oxalic acid-treated limestone with Al<sub>2</sub>O<sub>3</sub> and later decays over the 20 carbonation-calcination cycles. The oxalic acid-treated limestone with Al<sub>2</sub>O<sub>3</sub> has low surface area which can lead to low CO<sub>2</sub> adsorption capacity (Younas et al., 2016). After normalizing the CO<sub>2</sub> uptake capacity based on the first cycle, treated limestone with oxalic acid appears to be the most stable material in TGA cycling experiment. From this result, fresh Malaysian limestone is found to have higher CO<sub>2</sub> uptake capacity after 20 cycles which is 0.396 g CO<sub>2</sub>/g limestone than limestone reported by Sun et al., 2016 which is 0.220 g CO<sub>2</sub>/g limestone.

**Figure 5A** shows that completely closed carbon balance has been achieved over all 100 cycles, suggesting the high accuracy, high precision and good consistency of the experimental measurements. CO<sub>2</sub> uptake capacity over 100 cycles of carbon capture is depicted in **Figure 5B**. The capture capacities measured by the fluidized bed reactor experiments appear two orders of magnitudes higher than that measured by the TGA (see **Figure 4**), despite the latter using much smaller particle sizes. This may be attributed to the significantly faster external mass transfer rate in a fluidized bed reactor. Both the TGA and the fluidized bed experiments agree that the initial CO<sub>2</sub> capture capacity of non-treated limestone and oxalic acid-treated limestone is higher than oxalic acid-treated limestone with Al<sub>2</sub>O<sub>3</sub>. This suggests that limestone type and origin could also be a factor that influences the final properties of the modified sorbent. However, unlike in the TGA, the CO<sub>2</sub> uptake capacities of non-treated and oxalic acid-treated limestone decay much faster in fluidized bed.

**Figures 6A,B** show the pelletized samples before and after 100 carbonation-calcination cycles, respectively. The smaller particle sizes were exhibited after 100 carbonation-calcination cycles due to the extent of fragmentation occurred and the particle's corner also become more rounded due to the extent of attrition. However, the condition and shape of non-treated and oxalic acid-treated limestone show minor changes before and after 100 cycles proving the lack of mass loss as per **Table 4**.

**Table 4** shows the mass of the sorbents after 100 carbon capture cycles. The non-treated limestone and oxalic acid-treated



limestone have highest attrition resistance since they show the least fractional mass loss. The lack of mass loss in non-treated limestone and oxalic acid-treated limestone also suggests that their deactivation measured in the fluidized bed must be of microscopic nature, e.g. sintering. The lack of attrition resistance on oxalic acid-treated limestone with Al<sub>2</sub>O<sub>3</sub> attributes to the deactivation during the carbonation-calcination cycles. However, the CO<sub>2</sub> uptake capacity of oxalic acid-treated limestone appears to have stabilized after 75 carbon capture cycles (see **Figure 5B**), with a residual capacity of 1 mmol CO<sub>2</sub>/g sorbent.

## Kinetic Analysis

From the TGA analysis and CO<sub>2</sub> capture studies, only oxalic acid-treated limestone was used to analyze the kinetic analysis due to its high CO<sub>2</sub> uptake capacity and its low fractional mass loss as shown in **Figure 5B** and **Table 4** respectively. Reaction rate and solid conversions as function of time, for both carbonation and calcination, at cycles 2, 10, 20, 50, and 100 are shown in **Figures 7, 8**, respectively. From **Figure 7**, the rate constant during carbonation almost falls linearly with conversion, suggesting a uniform nucleation mechanism. During calcination, the rate vs. solid conversion curve appears parabolic, suggesting that the

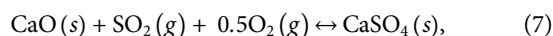
calcination reaction is somewhat autocatalytic. This observation is unsurprising given that the proceeding of the calcination reaction is often associated with pore opening and the subsequent increases in 1) pore size and 2) surface area. Both phenomena could result in the parabolic rate curves. The increase of time during the conversion of carbonation for cycle 2 as per shown in **Figure 8A** due to the lack of mass transfer of CO<sub>2</sub> diffused through the carbonation layer on the sorbent surface (Chou et al., 2018).

Based on the cyclic performance in the fluidized bed and the TGA, it is apparent that oxalic acid-treated limestone shows higher surface area and high CO<sub>2</sub> uptake capacity. Although these uptakes are higher than other limestone, they are still below expectation. The main finding of this work is the usage of Malaysian limestone as sorbent in calcium looping process and investigation of the CO<sub>2</sub> uptake capacity of this limestone. Then, the kinetic information obtained was used for the sizing and design of the carbonator and calciner reactors in the CCL process.

## Simulation of Calcium Carbonate Looping Process

The CCL process, was simulated based on the flue gas of the referenced plant using Aspen Plus simulator. The CCL process was divided into two process lines because of the large flow rate of the flue gas. Each process line had a carbonator reactor and two calciner reactors. A heat exchanger and a blower were installed before the carbonator reactor to ensure the temperature and pressure of the carbonator were maintained at 650 °C and 1 bar, respectively. Information on the flue gas before the carbonator reactor (for a single CCL process line) is shown in **Table 5**. Based on **Table 5**, the CO<sub>2</sub> gas fed to the carbonator reactor was 7,228.25 kmol/h (318.12 ton/h) per process line, which means that the total initial CO<sub>2</sub> gas emitted by the existing coal-fired power plant was 14,456.50 kmol/h (636.23 ton/h).

The presence of SO<sub>2</sub> in the carbonator reactor caused the CaO to favor the reaction with SO<sub>2</sub> rather than with CO<sub>2</sub>. In addition to the main reaction of **Eq. 1**, side reactions also occurred in the carbonator reactor and are shown as **Eqs. 7, 8**.



By using the best sample from the experiment (sample 3), the simulation of the carbonator was carried out using Aspen Plus to determine the conversions of the reactions in **Eqs. 1, 7, 8**. A Gibbs reactor was used to ensure that the equilibrium conversion of the main reaction was considered during the simulation. The results of the simulation are displayed in **Table 3**. Based on the results, it was found that the carbonator reactor of the CCL process was able to remove up to 89% (566.44 ton/h) of CO<sub>2</sub> from the flue gas of the referenced plant. Hence, the integrated coal-fired power plant's current emission was around 69.79 ton/h of CO<sub>2</sub>. It is worth noting that the sorbent was fed in excess, as there were side reactions in the

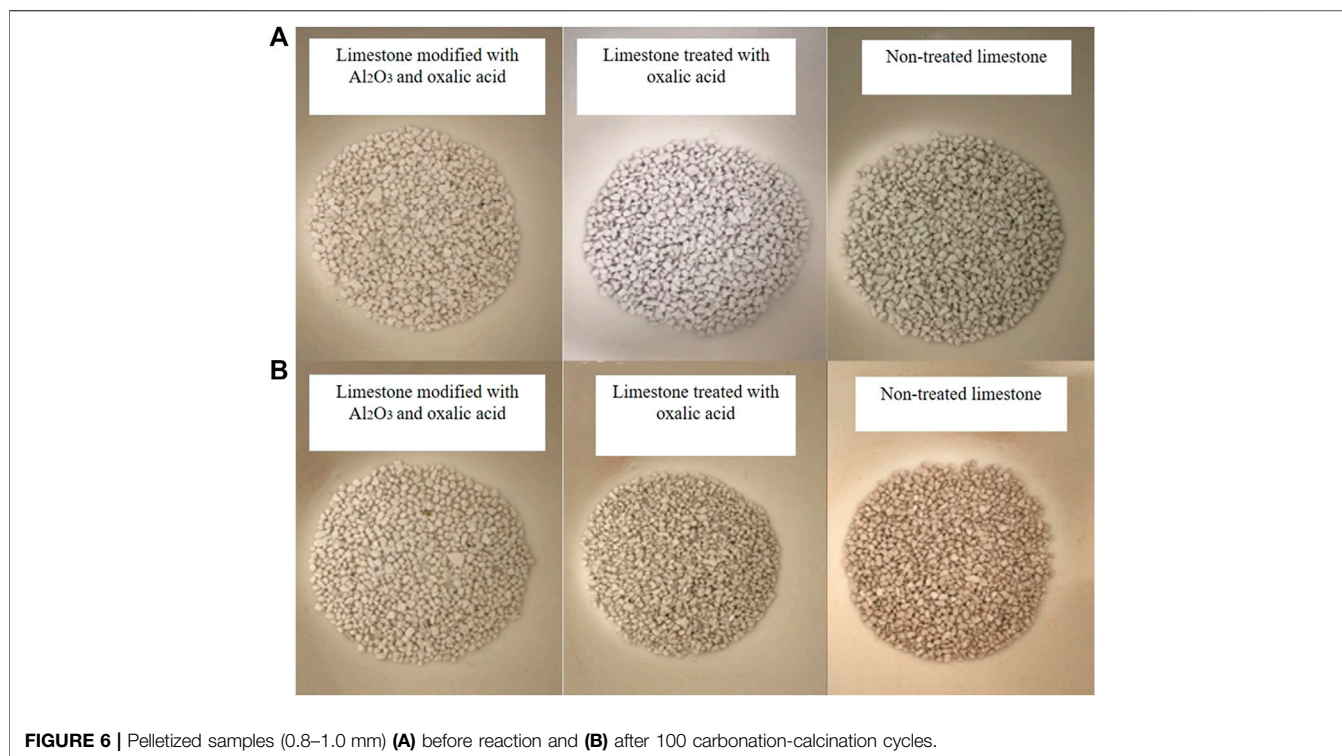


**FIGURE 6** | Pelletized samples (0.8–1.0 mm) **(A)** before reaction and **(B)** after 100 carbonation-calcination cycles.

**TABLE 3** | Reaction conversions in the carbonator reactor (single process line).

	Mole flowrate (kmol/hr)	Conversion (%)
CO	Inlet: 0.82	100.0
	Outlet: 0.0	
CO <sub>2</sub>	Inlet: 7,229.34	89.03
	Outlet: 792.89	
SO <sub>2</sub>	Inlet: 6.19	100.0
	Outlet: 0.0	

The number of cyclones used to achieve the desired efficiency was 12 (diameter = 3.4 m per cyclone) and 4 (diameter = 3.5 m per cyclone) for the carbonator and the calciner in each process line, respectively. From the simulation of the final calciner cyclone separator, the total make-up sorbent required was 70.51 kmol/h (7.06 ton/h) for each line. Hence, a total of 1.95% (0.011 mol/mol or 14.12 ton/h) of sorbent was recycled for the two CCL process lines. This value is much lower than the one in Michalski et al. (2019)'s work (3–7%) and Mantripragada and Rubin (2014)'s work (0.025 mol/mol).

**TABLE 4** | Mass of sorbents before and after 100 carbon capture cycles in a bubbling fluidized bed.

Sample name	Initial mass (g)	Final mass (g)	Fractional mass loss
Oxalic acid-treated limestone with Al <sub>2</sub> O <sub>3</sub>	0.89	0.68	0.23
Oxalic acid-treated limestone	1	0.95	0.05
Non-treated limestone	1	0.82	0.18

reactor. The total flow rate of the used sample 3 was 6,443.46 kmol/h (361.33 ton/h) for each process line.

For the calciner reactor, a simulation was carried out at the temperature and pressure used in the experiment, which were 920 °C and 1 bar, respectively. At these operating conditions, the solid CaCO<sub>3</sub> fed into the calciner reactor was fully converted back into sample 3. The only reaction considered in the calciner reactor was the main reaction of Eq. 1 since other components were separated in the cyclone separators with efficiencies of 99.5%. The Stairmand-High Throughput (Stairmand-HT) cyclone separator type was chosen because of the large flowrate handled by the cyclone separator.

## Economic Potential

A summary of the results from the economic analysis of the referenced plant with and without a CCL process is presented in Table 6. From the Aspen simulator, for each process line, the estimated heat usage ( $Q$ ) was around  $25.77 \times 10^4$  and  $18.40 \times 10^4$  kW for the carbonator and the calciner, respectively. The flow rate of the inlet gas ( $Q_g$ ) to each carbonator's cyclone separator was  $20.54 \times 10^4$  ft<sup>3</sup>/min whilst for each calciner's cyclone separator was  $19.13 \times 10^4$  ft<sup>3</sup>/min. The heat exchanger used in this study operated with a surface area ( $A_{Hex}$ ) of 63,675.35 m<sup>2</sup> and a pressure of around 1 bar. The



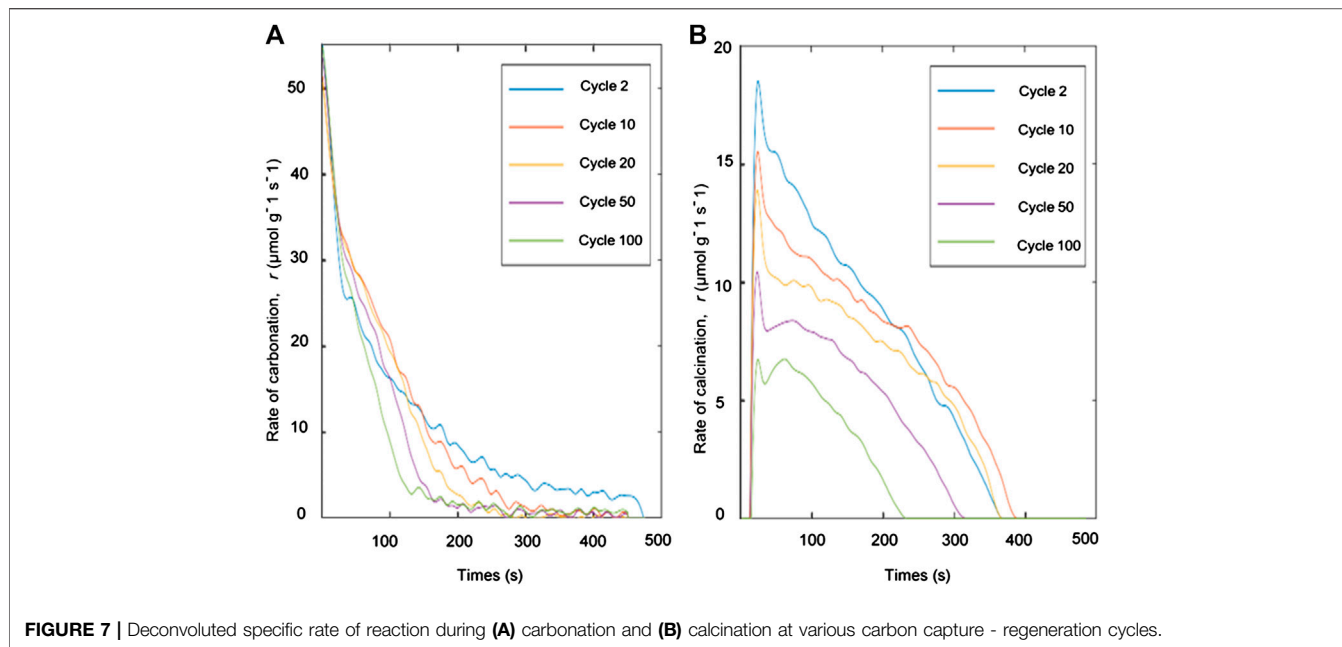


FIGURE 7 | Deconvoluted specific rate of reaction during (A) carbonation and (B) calcination at various carbon capture - regeneration cycles.

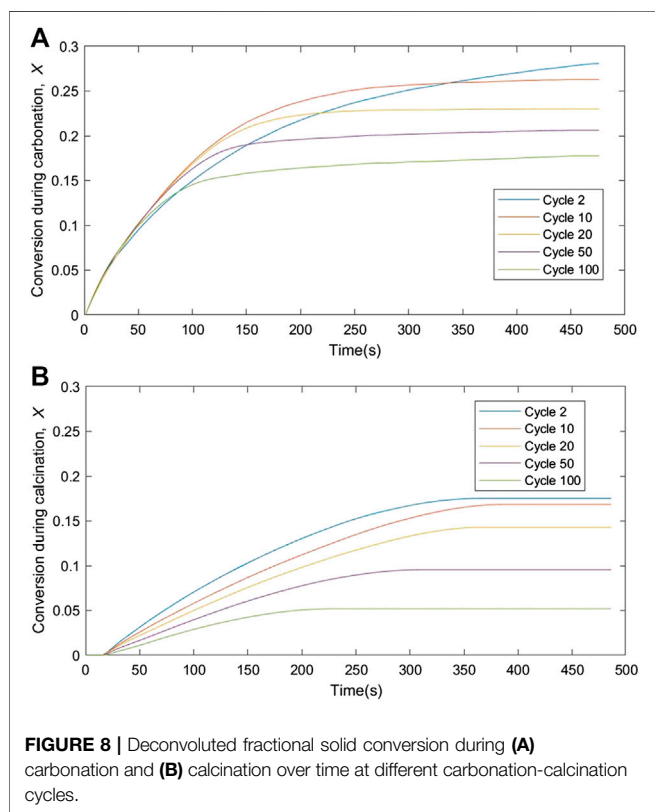


FIGURE 8 | Deconvoluted fractional solid conversion during (A) carbonation and (B) calcination over time at different carbonation-calcination cycles.

compressor used had a brake horsepower ( $P_B$ ) of 548.41 kW and an isentropic efficiency of 72%. The total capital cost of the major pieces of equipment was estimated based on this information and Eqs. 2–6.

TABLE 5 | Carbonator reactor's feed information (single process line).

Feed type	Parameter	Value
Flue gas	Flow (kmol/hr)	60,997.89
	Temperature (°C)	650
	Pressure (bar)	1.0
	Content (mol%)	
	CO <sub>2</sub>	11.85
	H <sub>2</sub> O	25.33
	O <sub>2</sub>	4.10
	N <sub>2</sub>	58.67
	NO	0.04
	SO <sub>2</sub>	0.01

TABLE 6 | Economics of the referenced plant with and without the CCL process.

	Without CCL process	With CCL process
Total capital cost (M USD)	1,539.11	2,942.66
CCL capital cost (M USD)	—	1,403.55
Total operation cost (M USD/yr)	183.99	310.12
CCL operation cost (M USD/yr)	—	126.13
Specific CO <sub>2</sub> emission, kg/MWh	909.03	99.70

The operating cost was estimated based on the coal consumption and the prices of coal, sorbents and cooling water, which were USD 2.73/GJ (Rolfe et al., 2018), USD 25.76/ton (Mantripragada and Rubin, 2014), and USD 0.354/GJ (Yu and Chien, 2016), respectively. The operating hours of the integrated plant were assumed to be 8,078 h/yr. The amounts of the materials and utilities used in the CCL plant were retrieved from the Aspen simulator. They consisted of 662.42 GJ/h of coal,

7.06 ton/h of make-up sorbents and 85.92 GJ/h of cooling water for each process line.

The results show that the total capital cost of the referenced plant is 1,539.11 M USD and an additional cost of 1,403.55 M USD is required to integrate the CCL process with the referenced plant. The high operating cost of the integrated plant is due to the requirement of additional coal as fuel for the heat supply of the calciner reactor. In addition, make-up sorbent of around 14.12 ton/h also contributes to the increase in operating cost. Despite that, the amount of CO<sub>2</sub> released from the plant is significantly reduced, from 909 to 99.7 kg/MWh. The specific CO<sub>2</sub> emission of the integrated plant is lower than those in previous studies (OECD, 2011; Michalski et al., 2019).

## CONCLUSION

A study on the performance and process modeling of a 700 MWe coal-fired power plant integrated with a calcium carbonate looping process that uses oxalic-acid treated limestone was successfully carried out. The CO<sub>2</sub> uptake capacity and performance of Malaysian limestone treated with oxalic acid shows the highest value compare to non-treated limestone and oxalic acid-treated limestone with aluminum oxide (Al<sub>2</sub>O<sub>3</sub>) as supporting materials, due to higher attrition resistance. Although the CO<sub>2</sub> uptakes are higher than other limestone, they are still below expectation. The main finding of this work is the usage of Malaysian limestone as sorbent in calcium looping process and investigate the CO<sub>2</sub> uptake capacity of this limestone. Through Aspen Plus simulations, CO<sub>2</sub> emissions of up to 89% (from 909 to 99.7 kg/MWh) was able to be

reduced when the integrated plant was used. Make-up sorbent of around 14.12 ton/h was required for the integrated plant. The make-up sorbent became one of the major contributors to the high operation cost of the calcium carbonate looping process. Hence, further study may be carried out in the future to further improve the CO<sub>2</sub> uptake capacity of the oxalic acid-treated limestone by integrating the limestone with different types of supporting material, which may lead to lower capital and operation costs due to lower sorbent usage and make-up required.

## DATA AVAILABILITY STATEMENT

The original contributions presented in the study are included in the article/Supplementary Material, further inquiries can be directed to the corresponding author.

## AUTHOR CONTRIBUTIONS

All authors listed have made a substantial, direct, and intellectual contribution to the work and approved it for publication.

## FUNDING

This work was financially supported by Ministry of Higher Education Malaysia (MOHE) under the Fundamental Research Grant Scheme (FRGS), UNITEN Sdn. Bhd. under the Bold Grant (10436494/B/2019141), and UNITEN R&D Sdn. Bhd. under the Seeding Fund (U-TG-RD-18-28).

## REFERENCES

- Abeysdeera, U. W., Hewage, L., Mesthrige, J. W., and Samarasinghalage, T. I. (2019). Global research on carbon emissions: a scientometric review. *Sustainability* 11 (14), 3972. doi:10.3390/su11143972
- Akerboom, S., Botzen, W., Buijze, A., Michels, A., and van Rijswijk, M. (2020). Meeting goals of sustainability policy: CO<sub>2</sub> emission reduction, cost-effectiveness and societal acceptance. An analysis of the proposal to phase-out coal in the Netherlands. *Energy Pol.* 138, 111210. doi:10.1016/j.enpol.2019.111210
- Anderson, S., and Newell, R. (2004). Prospects for carbon capture and storage technologies. *Annu. Rev. Environ. Resour.* 29, 109–142. doi:10.1146/annurev.energy.29.082703.145619
- Arias, B., Diego, M. E., Abanades, J. C., Lorenzo, M., Diaz, L., Martinez, D., et al. (2013). Demonstration of steady state CO<sub>2</sub> capture in a 1.7 MWth calcium looping pilot. *Int. J. Greenh. Gas Control.* 18, 237–245. doi:10.1016/j.ijggc.2013.07.014
- Benitez-Guerrero, M., Valverde, J. M., Schanez-Jimenez, P. E., Perejon, A., and Perez-Maqueda, L. A. (2018). Calcium Looping performance of mechanically modified Al<sub>2</sub>O<sub>3</sub>-CaO composites for energy storage and CO<sub>2</sub> capture. *Chem. Eng. J.* 334, 2343–2355. doi:10.1016/j.cej.2017.11.183
- Carpenter, S. M., Henry, A., and Long (2017). *Integrated Gasification combined cycle (IGCC) technologies*. Sawston, United Kingdom: Woodhead Publishing, 445–465. doi:10.1016/B978-0-08-100167-7.00036-6
- Chang, M. H., Huang, C. M., Liu, W. H., Chen, W. C., Cheng, J. Y., Chen, W., et al. (2013). Design and experimental investigation of calcium looping process for 3 and 1.9-MWth facilities. *Chem. Eng. Technol.* 36 (9), 1525–1532. doi:10.1002/ceat.201300081
- Charitos, A., Hawthorne, C., Bidwe, A. R., Sivalingam, S., Schuster, A., Spliethoff, H., et al. (2010). Parametric investigation of the calcium looping process for CO<sub>2</sub> capture in a 10 kWth dual fluidised bed. *International Journal of Greenhouse Gas Control* 4 (5), 776–784. doi:10.1016/j.ijggc.2010.04.009
- Chou, Y. C., Cheng, J. Y., Liu, W. H., and Hsu, H. W. (2018). Effects of steam addition during calcination on carbonation behavior in a calcination/carbonation loop. *Chem. Eng. Technol.* 41 (10), 1921–1927. doi:10.1002/ceat.201800133
- Cui, L., Li, R., Song, M., and Zhu, L. (2019). Can China achieve its 2030 energy development targets by fulfilling carbon intensity reduction commitments?. *Energy Econ.* 83, 61–73. doi:10.1016/j.eneco.2019.06.016
- Erans, M., Jeremias, M., Zheng, L., Yao, J. G., Blamey, J., Manovic, V., et al. (2018). Pilot testing of enhanced sorbents for calcium looping with cement production. *Appl. Energy* 225, 392–401. doi:10.1016/j.apenergy.2018.05.039
- Fedunik-Hofman, L., Bayon, A., and Donne, S. W. (2019). Comparative kinetic analysis of CaCO<sub>3</sub>/CaO reaction system for energy storage and carbon capture. *Appl. Sci.* 9 (21), 4601. doi:10.3390/app9214601
- Florin, N., and Fennell, P. (2011). Synthetic CaO-based sorbent for CO<sub>2</sub> capture. *Energy Procedia* 4, 830–838. doi:10.1016/j.egypro.2011.01.126
- Hilz, J., Haaf, M., Helbig, M., Lindqvist, N., Ströhle, J., and Epple, B. (2019). Scale-up of the carbonate looping process to a 20 MWth pilot plant based on long-term pilot tests. *Int. J. Greenh. Gas Control.* 88, 332–341. doi:10.1016/j.ijggc.2019.04.026
- Hou, S. S., Chiang, C. Y., and Lin, T. H. (2020). Oxy-fuel combustion characteristics of pulverized coal under O<sub>2</sub>/recirculated flue gas atmospheres. *Appl. Sci.* 10, 1362. doi:10.3390/app10041362
- International Energy Agency (2016a). *Energy, climate change and environment: 2016 insights*. Paris, France: IEA.
- International Energy Agency (2016b). *Key world energy statistics 2016*. Paris, France: IEA.

- Li, Y., Zhao, C., Chen, H., Liang, C., Duan, L., and Wu, Z. (2009). Modified CaO-based sorbent looping cycle for CO<sub>2</sub> mitigation. *Fuel* 88, 697–704. doi:10.1016/j.fuel.2008.09.018
- Mantripragada, H. C., and Rubin, E. S. (2014). Calcium looping cycle for CO<sub>2</sub> capture: performance, cost and feasibility analysis. *Energy Procedia* 63, 2199–2206. doi:10.1016/j.egypro.2014.11.239
- Michalski, S., Hanak, D. P., and Manovic, V. (2019). Techno-economic feasibility assessment of calcium looping combustion using commercial technology appraisal tools. *J. Clean. Prod.* 219, 540–551. doi:10.1016/j.jclepro.2019.02.049
- Miranda-Pizarro, J., Perejón, A., Valverde, J. M., Pérez-Maqueda, L. A., and Sánchez-Jiménez, P. E. (2017). CO<sub>2</sub> capture performance of Ca-Mg acetates at realistic Calcium Looping conditions. *Fuel* 196, 497–507. doi:10.1016/j.fuel.2017.01.119
- Mutch, G. A., Anderson, J. A., and Vega-Maza, D. (2017). Surface and bulk carbonate formation in calcium oxide during CO<sub>2</sub> capture. *Appl. Energy* 202, 365–376. doi:10.1016/j.apenergy.2017.05.130
- OECD (2011). *Carbon pricing, power markets and the competitiveness of nuclear power*. Paris, France: OECD Publishing.
- Przekop, R. E., Marciniak, P., Sztorch, B., Czapiak, A., Stodolny, M., and Martyla, A. (2018). New Method for the synthesis of Al<sub>2</sub>O<sub>3</sub>-CaO and Al<sub>2</sub>O<sub>3</sub>-CaO-CaCO<sub>3</sub> systems from a metallic precursor by the sol-gel route. *J. Aust. Ceram. Soc.* 54, 679–690. doi:10.1007/s41779-018-0197-0
- Radfarnia, H. R., and Iliuta, M. C. (2013). Metal oxide-stabilised calcium oxide CO<sub>2</sub> sorbent for multicycle operation. *Chem. Eng. J.* 232, 280–289. doi:10.1016/j.ccej.2013.07.049
- Ramezani, M., Tremain, P., Doroodchi, E., and Moghtaderi, B. (2017). Determination of carbonation/calcination reaction kinetics of a limestone sorbent in low CO<sub>2</sub> partial pressures using TGA experiments. *Energy Procedia* 114, 259–270. doi:10.1016/j.egypro.2017.03.1168
- Ramkumar, S., and Fan, L. S. (2010). Thermodynamic and experimental analyses of the three-stage calcium looping process. *Ind. Eng. Chem. Res.* 49 (16), 7563–7573. doi:10.1021/ie100846u
- Ridha, F. N., Manovic, V., Macchi, A., Anthony, M. A., and Anthony, E. J. (2013). Assessment of limestone treatment with organic acids for CO<sub>2</sub> capture in Ca-looping cycles. *Fuel Process. Technol.* 116, 284–291. doi:10.1016/j.fuproc.2013.07.007
- Rolfe, A., Huang, Y., Haaf, M., Rezvani, S., McIveen-Wright, D., and Hewitt, N. J. (2018). Integration of the calcium carbonate looping process into an existing pulverised coal-fired power plant for CO<sub>2</sub> capture: techno-economic and environmental evaluation. *Appl. Energy* 222, 169–179. doi:10.1016/j.apenergy.2018.03.160
- Seider, W. D., Seader, J. D., Lewin, D. R., Widagdo, S., Gani, R., and Ng, K. M. (2019). *Product and process design principles: synthesis, analysis and design*. Hoboken, NJ: John Wiley & Sons.
- Sinnott, R., and Towler, G. (2020). *Chemical engineering design*. SI Edition. Oxford, United Kingdom: Butterworth-Heinemann.
- Stendardo, S., Andersen, L. K., and Herce, C. (2013). Self-activation and effect of regeneration conditions in CO<sub>2</sub>-carbonate looping with CaO–Ca<sub>12</sub>Al<sub>14</sub>O<sub>33</sub> sorbent. *Chem. Eng. J.* 220, 383–394. doi:10.1016/j.ccej.2013.01.045
- Ströhle, J., Orth, M., and Epple, B. (2015). Chemical looping combustion of hard coal in a 1 MWth pilot plant using ilmenite as oxygen carrier. *Appl. Energy* 157, 288–294. doi:10.1016/j.apenergy.2015.06.035
- Sun, R., Li, Y., Liu, H., Wu, S., and Lu, C. (2012). CO<sub>2</sub> capture performance of calcium-based sorbent doped with manganese salts during calcium looping cycle. *Appl. Energy* 89 (1), 368–373. doi:10.1016/j.apenergy.2011.07.051
- Sun, R., Liu, W., Li, M., Yang, X., Wang, W., Hu, Y., et al. (2016). Mechanical modification of naturally occurring limestone for high temperature CO<sub>2</sub> capture. *Energy & Fuels* 30 (8), 6597–6605. doi:10.1021/acs.energyfuels.6b01131
- Valverde, J. M., Barea-Lopez, M., Perejon, A., Sanchez-Jimenez, P. E., and Perez-Maqueda, L. A. (2017). Effect of thermal pretreatment and nanosilica addition on limestone performance at calcium-looping conditions for thermochemical energy storage of concentrated solar power. *Energy & Fuels* 31 (4), 4226–4236. doi:10.1021/acs.energyfuels.6b03364
- Wang, Y., Zhao, L., Otto, A., Robinius, M., and Stolten, D. (2017). A review of Post combustion CO<sub>2</sub> capture Technologies from. *Coal-Fired Power Plant* 114, 650–665. doi:10.1016/j.egypro.2017.03.1209
- Xiong, Y. Q., Luo, P., and Hua, B. (2014). Energy consumption analysis of air separation process for oxy-fuel combustion system. *Adv. Mater. Res.* 1033, 146–150. doi:10.4028/www.scientific.net/AMR.1033-1034.146
- Younas, M., Sohail, M., Leong, L. K., and Sumathi, S. (2016). Feasibility of CO<sub>2</sub> adsorption by solid adsorbents: a review on low temperature systems. *Int. J. Environ. Sci. Technol.* 13, 1839–1860. doi:10.1007/s17362-016-1008-1
- Yu, B. Y., and Chien, I. L. (2016). Design and optimisation of the methanol-to-olefin process. Part I: steady-state design and optimization. *Chem. Eng. Technol.* 39 (12), 2293–2303. doi:10.1002/ceat.201500654
- Zhang, Z., Zhang, A., Wang, D., Li, A., and Song, H. (2017). How to improve the performance of carbon tax in China? *J. Clean. Prod.* 142, 2060–2072. doi:10.1016/j.jclepro.2016.11.078
- Zhou, L., Duan, L., and Anthony, E. J. (2019). A calcium looping process for simultaneous CO<sub>2</sub> capture and peak shaving in a coal-fired power plant. *Appl. Energy* 235, 480–486. doi:10.1016/j.apenergy.2018.10.138

**Conflict of Interest:** The authors declare that the research was conducted in the absence of any commercial or financial relationships that could be construed as a potential conflict of interest.

Copyright © 2021 Zubir, Afandi, Manap, Hamid, Ayodele, Liu and Abd Hamid. This is an open-access article distributed under the terms of the Creative Commons Attribution License (CC BY). The use, distribution or reproduction in other forums is permitted, provided the original author(s) and the copyright owner(s) are credited and that the original publication in this journal is cited, in accordance with accepted academic practice. No use, distribution or reproduction is permitted which does not comply with these terms.